LAWRENCE
LIVERMORE
NATIONAL
LABORATORY

LLNL-JRNL-454091

Backscatter Measurements for NIF Ignition Targets

J. D. Moody, P. Datte, K. Krauter, E. Bond, P. A. Michel, S. H. Glenzer, L. Divol, C. Niemann, L. Suter, N. Meezan, B. J. MacGowan, R. Hibbard, R. London, J. Kilkenny, R. Wallace, J. L. Kline, K. Knittel, G. Frieders, B. Golick, G. Ross, K. Widmann, J. Jackson, S. Vernon, T. Clancy

September 9, 2010

Review of Scientific Instruments

Disclaimer

This document was prepared as an account of work sponsored by an agency of the United States government. Neither the United States government nor Lawrence Livermore National Security, LLC, nor any of their employees makes any warranty, expressed or implied, or assumes any legal liability or responsibility for the accuracy, completeness, or usefulness of any information, apparatus, product, or process disclosed, or represents that its use would not infringe privately owned rights. Reference herein to any specific commercial product, process, or service by trade name, trademark, manufacturer, or otherwise does not necessarily constitute or imply its endorsement, recommendation, or favoring by the United States government or Lawrence Livermore National Security, LLC. The views and opinions of authors expressed herein do not necessarily state or reflect those of the United States government or Lawrence Livermore National Security, LLC, and shall not be used for advertising or product endorsement purposes.

Backscatter measurements for NIF ignition targets

J. D. Moody, P. Datte, K. Krauter, E. Bond, P. A. Michel, S. H. Glenzer, L. Divol, C. Niemann[1], L. Suter, N. Meezan, B. J. MacGowan, R. Hibbard, R. London, J. Kilkenny, R. Wallace, J. L. Kline[2], K. Knittel, G. Frieders, B. Golick, G. Ross, K. Widmann, J. Jackson, S. Vernon, and T. Clancy

*Lawrence Livermore National Laboratory, P. O. Box 808, Livermore, CA 94550**

[1] Physics Department, University of California Los Angeles, Los Angeles, CA 90095 USA. and

[2] Los Alamos National Laboratory, Los Alamos, NM USA.

(Dated: August 30, 2010)

Backscattered light via laser-plasma instabilities (LPI) has been measure in early NIF hohlraum experiments on two beam quads using a suite of detectors. A FABS (Full Aperture Backscatter System) and NBI (Near Backscatter Imager) instrument separately measure the stimulated Brillouin (SBS) and stimulated Raman scattered (SRS) light. Both instruments work in conjunction to determine the total backscattered power to an accuracy of ∼15%. In order to achieve the power accuracy we have added time-resolution to the NBI for the first time. This capability provides a temporally resolved spatial image of the backscatter which can be viewed as a movie.

I. INTRODUCTION

Experiments on the path toward achieving thermonuclear fusion have recently begun[1] on the National Ignition Facility (NIF)[2]. Reaching ignition relies on meeting high performance requirements for both the laser and target. The indirect drive ignition target has a smooth deuterium-tritium ice layer on the inside of a fuel capsule which is suspended in the center of a gold cylinder or hohlraum. Symmetric laser illumination on the inner wall fills the hohlraum with x-rays which ablate the fuel capsule compressing it and causing it to reach densities and temperatures which initiate nuclear fusion and burn of the fuel[3]. Frequency tripled (351 nm) laser beams provide up to 1.8 MJ of energy to the target with about 10% of this coupled into the fuel capsule[4].

Progress toward ignition requires a strategic set of diagnostic instruments suited to measure the performance of the laser and target. The first series of experiments on indirect drive hohlraum targets has focused on characterizing the energy loss through backscatter and selecting laser and target properties that limit this loss to less than about 10% total. This paper describes the set of instruments used to make measurements of optical backscattered light from NIF targets. The backscatter diagnostic builds off of similar instruments installed on other laser systems such as Nova[5], Omega[6, 7], and early light measurements on NIF[8–12].

Figure 1 shows that the NIF backscatter instrument consists of three systems. The Full Aperture Backscatter System (FABS) provides power time history and temporally resolved spectral measurements of light backscattered into the incident aperture. The Near Backscatter Imaging system (NBI) measures light scattered outside of the FABS aperture which extends out to a cone angle corresponding to about an f/4.7. A large scatter plate surrounding the incident aperture is mounted inside the target chamber. This plate is viewed with gated ICCD cameras which record 2-D images of the time-integrated

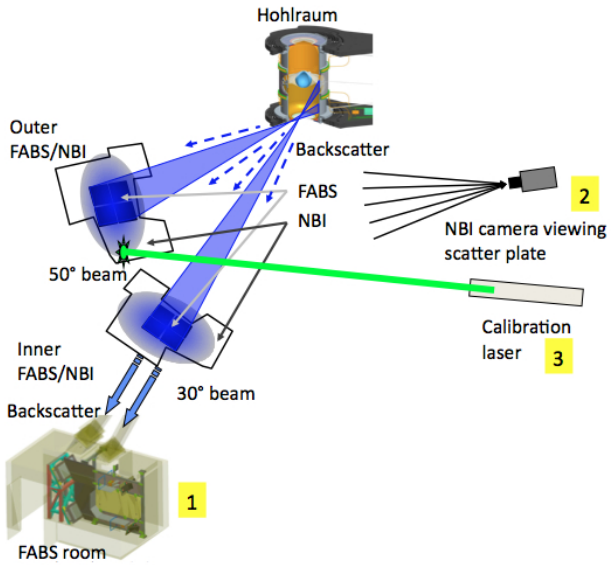

FIG. 1. The backscatter system consists of a 1) FABS instrument and 2) NBI instrument for two NIF quads, and a 3) Pulsed laser calibration instrument.

light distribution on the scatter plate. A new time-resolved measurement capability has been added to the NBI. This instrument uses 40 optical fibers and an optical streak camera to record the time history of light intensity at many points on the scatter plate. After normalization the data is assembled into a movie showing the evolving light distribution pattern. This movie contains the quantitative information for determining the complete time-resolved backscatter behavior. Both the FABS and NBI systems make separate measurements for light in two independent spectral bands. One band corresponds to the Stimulated Brillouin Scattering (SBS, 350 nm to 353 nm, produced by ion acoustic plasma waves) and the other to Stimulated Raman Scattering (SRS, 450 nm to 750 nm produced by Langmuir plasma waves). Figure 2 (b) shows the time-integrated SRS light from a

hohlraum shot recorded on the NBI. There is a region between the FABS and NBI that is not measured and there are cutouts on the scatter plate where no measurement is made. Interpolation and extrapolation methods in the data analysis provide an approximate reconstruction of this missing data. Interpolation is also used to fill in the FABS region and generate the image shown. Comparing the NBI-interpolated FABS with the measured FABS provides self-verification of the instruments. The backscatter system includes other forms of redundancy and self-checking capability to verify error and provide some level of backup if any instruments miss data. Table I lists the major requirements for the backscatter system.

TABLE I. Backscatter system requirements

Measurement	Requirement value
Power accuracy	15% error at 15% scatter[a]
Time resolution	0.4 ns
SBS spectral res.	0.06 nm
SRS spectral res.	5 nm

[a] At 5% backscatter the allowed error is 25% and at 2% backscatter the allowed error is 50%.

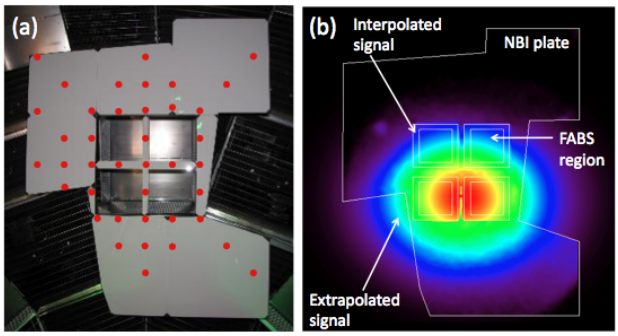

FIG. 2. (a) NBI scatter plate shown in the target chamber. Also shown are the locations viewed by the fibers in the time-resolved NBI system (b) Time-integrated SRS backscattered light from a cryo hohlraum target illuminates the lower-center region of the plate.

The organization of the remainder of this paper is as follows. Section II describes the FABS, Section III describes the NBI, Section IV describes the calibration system and error estimates. Section V gives a summary and conclusion.

II. FABS

The FABS instrument measures the energy, power, and spectra of the backscattered light from the target collected by the incident light aperture. Figure 3 shows one beamline of the FABS. There are two FABS on NIF and each one is designed to measure the backscatter on a 2-by-2 set of 4 beams called a "quad." One FABS is placed on an "inner" beam cone (30° from the hohlraum axis) and the other is on an "outer" beam cone (50° from the axis). Infrared laser power (at 1053 nm) is directed by the final laser turning mirror (LM8) through the frequency conversion crystals where it is converted to UV (351 nm). It then propagates through a phase plate, a polarization rotator, and the wedge focus lens (WFL) which focuses the UV light onto the target. The inner cone beams propagate further into the hohlraum before reaching the wall as compared to the outer beams. The backscattered light propagates back up the beam line, transmits through the LM8 and enters the FABS instrument.

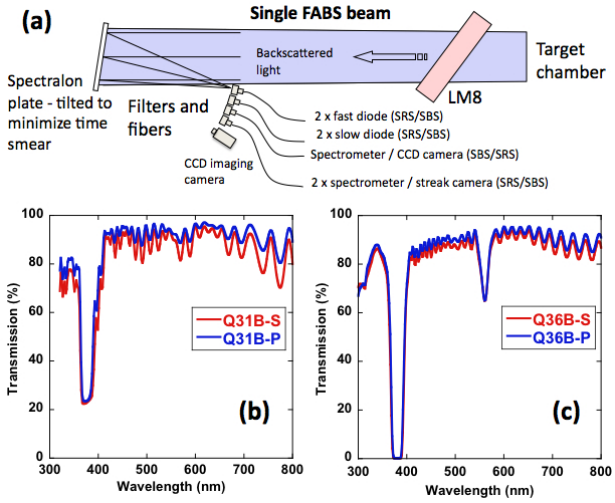

FIG. 3. (a) Sketch of the FABS system showing light passing from the target through the final laser turning mirror and onto the spectralon diffuser plate. Eight fiber-fed instruments measure different aspects of the light. (b) Measured S and P polarization transmission through the LM8 mirrors used for FABS-31 and (c) for FABS-36. The transmission dip in FABS-36 at 560 nm is corrected in the diodes with a special filter.

A significant challenge to measuring backscattered light on large laser systems is that there is too much light. A large fraction of it must be thrown away before it reaches the detectors. This is accomplished in FABS by directing the light to a Spectralon diffuser and collecting a fraction of the scattered light with a 400μm fiber placed 2.5 m away. The collected light fraction is given by $(r/R)^2 = (0.02/250)^2 = 6.4\times10^{-9}$. The Spectralon has a measured damage threshold of about 3 J/cm^2[11] which corresponds to about 70% backscatter on a 1 megajoule shot.

Four of the fiber pickoffs measure SBS signals and the other four measure SRS signals. Filters placed in front of the fibers select the wavelength band of interest, tailor the wavelength transmission to make some of the detectors "color-blind", and attenuate the light coupled to the fibers.

Mitsubishi step-index fiber [ST400E] is used exclu-

sively in the FABS system. This is 400 μm core diameter fused silica fiber that has better transmission in the UV than the graded index version of the same fiber. The fiber lengths were chosen to minimize the modal and chromatic dispersion[13] and still meet the required ≤ 0.4 ns temporal resolution.

II (a). FABS diodes and filters

Hamamatsu R1328U-53MOD fast phototubes with an extended S-20 photocathode measure the calibrated power time-history of both the SRS and SBS. These diodes have an intrinsic response time of 60 to 80 ps. Output signal from the diode is coupled to a high-bandwidth coax cable (LMR600) of about 40 m length which carries the signal to a fast Tektronix DPO70404 scope. Dispersion in the long cable can be corrected in the data analysis.

The slow diodes provide a calibrated measure of the energy (redundant with integrating the fast diode signal) although they can also provide a slow time-response power measurement. The diodes are Electro-Optic Technology Inc.[15] ET-2020 biased detectors with a time response of about 2.5 - 3 ns. The signal from two diodes is multiplexed onto a single channel of a Tektronix DPO7104 scope with a 100 ns time separation. This timing difference is achieved with an additional 20 m of fiber.

Precision *in-situ* calibration of the diodes is done using a pulsed laser from TCC. This is described in detail in Section IV. A separate measure of the diode coupling to the Spectralon plate (without the effect of the beam line transmission) provides a useful check that the system is working as expected. The measured fast diode coupling ranges from about 2.3×10^{-9} V/W to 5.1×10^{-9} V/W over the four beams. The slow diode coupling ranges from 7×10^{-9} V/W to 7×10^{-8} V/W.

The photodiodes have wavelength-dependent response characteristics. Using them as stand-alone instruments requires the use of a "flattening" filter which adjusts the color sensitivity of the diode making it "color blind" to light from TCC. This removes the need to perform post-shot analysis relying on temporally-resolved spectral information. The resulting diode data can be converted to SRS power /energy by a single scale factor. Advanced Thin Films[14] built the flattening filters for the fast and slow SRS diodes in FABS and for the SRS cameras for the NBI.

The SRS and SBS wavelength bands are selected with bandpass filters. The SBS filter transmits 60% at 351 nm and has a width of 50 nm. The SRS filter transmits 98% of the light in the range of 450 nm to 750 nm and drops to 10^{-5} outside of this range.

Metallic ND filters are used to attenuate light reaching the fibers because they can have a nearly wavelength independent transmission from 450 nm to 750 nm. Etalon effects of multiple metallic filters are mitigated by tilting the filters at alternating + and − 10° relative to the normal filter orientation.

II (b). Spectral measurements

A time-integrated calibration spectrometer provides the primary calibrated energy measurement for FABS. Eight fibers transport SRS and SBS light from each of the 4 beams of one FABS to the slit location of a McPherson 2035 spectrometer. This is an 0.35 m focal length spectrometer with a 100 l/mm grating giving a measured dispersion at the output of 29.4 nm/mm. The 400 μm diameter fibers are apertured with a 200 μm slit and are stacked vertically at the input. The output of the spectrometer is imaged onto a PI-Max gated ICCD camera (model 7361-0001) which is gated at 50 ns in order to gate out light that is not part of the main backscatter signal. The light is dispersed in first order for the SRS band and in second order for the SBS band. This instrument is absolutely calibrated using a Xe lamp at target chamber center (TCC).

The SRS and SBS time-resolved spectra are measured with a spectrometer-streak camera combination. Each spectrometer multiplexes the fiber signals from four beam lines, in a way described in[13]. Two of the four fibers are delayed 15 ns relative to the others in order to displace them in time on the streak. A typical streak record is shown in Fig. 4 (a). The SRS measurements utilize an Acton SP2150i spectrometer (1/5-meter) with a 150 l/mm grating giving a measured dispersion at the spectrometer output of 42.2 nm/mm. An LLNL (Lawrence Livermore National Lab) GSCP (Generic Streak Camera Platform) streak camera with an S-20 photocathode coupled to a CCD camera creates the streak record with a typical streak speed of 40 ns over the entire record. The CCD image is a 1365 x 1365 pixels. Chromatic dispersion in the fiber[13] causes red to arrive before blue. The delay is easily removed during analysis of the data. Figure 4 (b) shows a magnified image of the streak circled in Fig. 4 (a). The SRS shows amplitude modulations (AM) at 3 GHz which correlate with the incident laser modulations. The AM on the incident laser (pump) is ±4% and on the SRS the AM is ±12%. The backscatter level early in the pulse ($\sim$ 16 ns) is about 25%. Using a simple model for reflectivity which includes saturation the reflectivity (R) and gain (G) are related by: $\hat{R}[1 + \hat{s} - \hat{R}] = \hat{s} \exp(1 - \hat{R})GI/I_0$. Here, $\hat{R} = R\omega_0/\omega_1$, $\hat{s} = s\omega_0/\omega_1$, s is the seed, ω_0 is the pump frequency and ω_1 is the scattered light frequency. Using this to estimate G at $I = I_0$ gives $G \sim 26$. Estimating $\delta R/R$ from $\delta I/I_0$ at a gain of 26 says that $\delta R/R = 2.5\delta I/I_0$. Thus, a 4% pump AM should give a 10% AM in the reflectivity which is close to the measured 12%. This simple model is consistent for the backscatter level and AM measure-

ment and indicates that the SRS is in the partly saturated regime.

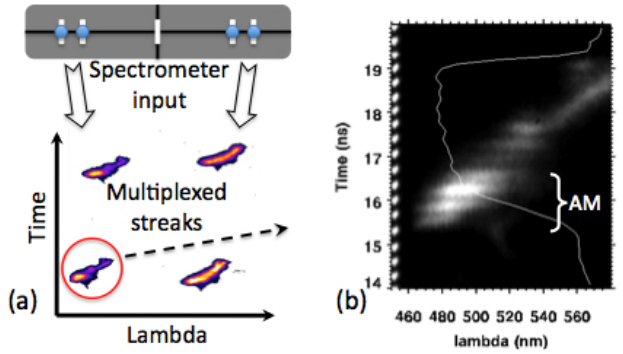

FIG. 4. Image shows the SRS spectra from the four beams on the 30° quad for a 1 MJ energy shot into a cryo hohlraum. All four spectra shows an increasing shift to the red with increasing time. Evidence of the amplitude modulation from the laser bandwidth (smoothing by spectral disperson) is visible in the lower left spectra. Also visible in the image on the left is the series of pulses from the comb generator.

Time-resolved spectral streaks of the SBS light are measured and multiplexed the same way as the SRS streaks. The SBS spectrometer is a McPherson 207 1-m spectrometer with a 2400 l/mm grating in second order for the 30° FABS and a McPherson 2061 3/4-meter spectrometer with a 2400 l/mm grating in second order for the 50° FABS. The measured dispersion for the 207 is 0.51 nm/mm and 0.37 nm/mm for the 2061. The streak camera is set to 40 ns across the streak record.

Figure 5 shows the SRS spectra summed over the 4 beams in the quad for two hohlraum shots. Shot 5 (a) is for a 500 kJ hohlraum with bare Au composing the laser entrance hole (LEH). Figure 5 (b) is scattering from a hohlraum with a 25 μm CH liner overcoated on the Au LEH. The purpose of the liner is to help slow the closing the LEH during the laser pulse as the Au plasma fills it in. The no-liner case has SRS at 13% and the liner has it at 29%. The spectra indicate that the laser beam does not propagate into as high of a density plasma when there is a liner. This result demonstrated that a hohlraum without liners is preferred for the ignition target.

III. NBI

The Near Backscatter Imager (NBI) system consists of a scatter plate mounted inside the target chamber and centered on a quad of beams and two viewing cameras, one for SRS and one for SBS. There are two of these instruments, one for each quad used for backscatter measurements. The purpose of the NBI is to measure light backscattered outside of the incident optics aperture. A new time-resolved NBI detector utilizes a distribution of

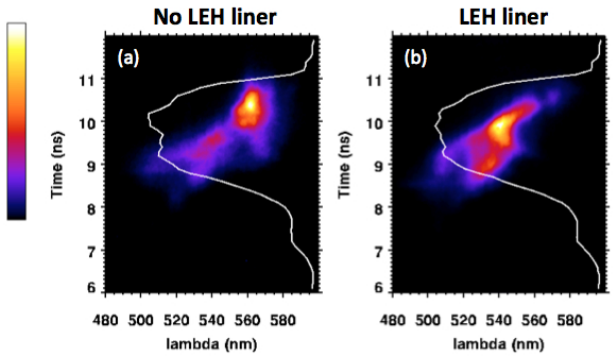

FIG. 5. The backscattered SRS spectrum summed over the 4 beams of the quad is shown for hohlraums with (a) pure Au for the LEH, (b) a 25μm LEH CH liner.

40 fibers and a streak camera to measure the time-history of the backscattered light spatial distribution on the scatter plate. This instrument can be configured to measure either SRS or SBS.

III (a). Scatter plate and detectors

Figure 2 (a) shows one scatter plate as seen in the NIF target chamber; both plates share the same design. The plates measure 1.5 m x 1.8 m and consist of protective borofloat glass on top of 7 mm thick spectralon which sits on a surface of aluminum held in place by a steel frame which is positioned with kinematic mounts. The plates have several cut-outs to avoid unconverted laser light from beams on the opposite side of the target chamber. A boundary plate and surface-mounted clips hold the glass and spectralon on the Al surface. All scatter plate metal with a view of the target is coated with 2μm B_4C to distribute the absorption of x-rays from the targets over a larger volume and reduce the possibility of metal ablation onto the scatter plate glass.

The ICCD cameras are PI-Max (model 7467-0022). A single camera pixel corresponds to about a 2.4 mm square on the plate. This gives about 16 pixels within the thin part of the "cross". The camera is gated for 50 ns to accommodate a range of laser pulse shapes. Signal from different parts of the plate arrives at different times due to the large spatial extent of the plate. The spread in this arrival time is approximately 5 ns and easily falls within the gate time of the camera. The f/stop for both cameras is set to f/16 and the image size is adjusted to fill as much of the CCD as possible.

The NBI optical filters are similar to the ones used for FABS. Bandpass filters select the SRS or SBS band. A flattening filter makes the SRS camera colorblind and metallic ND filters attenuate the signal.

III (b). Time-resolved NBI detector

The new time-resolved NBI instrument measures the time-history of the backscattered light distribution at selected points on the scatter plate. An optical system images the scatter plate onto a 400-μm fiber array outside the target chamber. These 400μm fibers pass through a taper where they reduce to 200μm and then travel 2 m and terminate in a linear array coupled to the input slit of a streak camera. Figure 2 (a) shows the scatter plate location seen by each fiber (red dots). Filters select either the SRS or SBS band, flatten the photocathode response of the streak camera, and attenuate the signal before it enters the fibers.

Light reaching the camera is streaked in time to give the temporal evolution of the light intensity at the 40 fiber locations on the plate. Analysis of the data produces a plot of W/cm^2 as a function of time at the fiber location on the scatter plate. Bi-linear interpolation is used to fill in the regions of the plate between the 40 points and create a snapshot of the backscattered spatial intensity distribution on the plate every 100 ps. These images are assembled into a movie which shows the temporally evolving backscattered light intensity on the NBI plate.

Figure 6 shows the time evolution of the NBI spatial distribution during the high-intensity part of the pulse for the experiment corresponding to Fig. 5 (b). The backscatter signal is deflected to the lower part of the plate and moves back toward the center at late times. The hohlraum experiments show that the temporal evolution of the total backscatter (FABS + NBI) is nearly identical to the time-history of the FABS signal. Comparisons of the NBI-time-resolved data with modeling are ongoing and will help verify that the hohlraum hydrodynamics and refraction of the SRS light are computed consistently with the experiment.

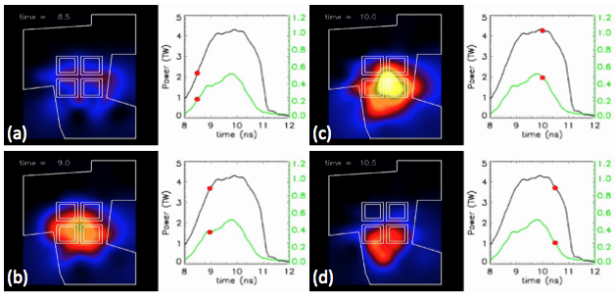

FIG. 6. Image shows the evolution of the spatial pattern on the NBI scatter plate for SRS. Stepping through the images in order the times are 8.5 ns, 9.0 ns, 10.0 ns, and 10.5 ns. The plots show the incident power (black) and the backscattered SRS power (green) with the marker on the curve indicating the time of the particular frame.

IV. CALIBRATION

Several techniques are utilized to demonstrate that the backscatter instruments meet the requirements given in Table I. Meeting these requirements is important for achieving an accurate understanding of the hohlraum energetics and providing specific experimental signatures that guide simulations of the hohlraum hydrodynamics.

IV (a). Spectral and temporal calibration

Mercury and Neon calibration lamps[18] provide sharp spectral lines used to measure the dispersion and offset wavelength of the SRS and SBS spectrometers. Target shots also produce scattered 351 nm and unconverted 527 nm light which provides periodic verification of the wavelength offsets.

The streaked spectral instruments and the fast diodes require identification of $t = 0$ relative to the laser pulse to an accuracy of 0.15 ns and the streaked instruments require calibration of the sweep rate. Timing shots establish the $t = 0$ for the instruments using a short 0.09 ns UV laser pulse on a flat gold disk. In addition to setting the $t = 0$, the streak cameras use a comb generator at 3 GHZ for an *in-situ* measure of their sweep speed.

IV (b). Power and energy calibration

The FABS calibration spectrometer is calibrated with a 300 W Oriel/Newport calibrated Xe lamp placed in the center of the target chamber. The calibration typically requires 10 minutes to obtain 3000 to 4000 counts per pixel for the SRS signal and provides the energy per nm per pixel-count for SRS and SBS on all four beamlines.

A Surelite laser (Continuum), capable of about 200 mJ of 532 nm and about 100 mJ of 355 nm laser light in a 4 ns Gaussian, is used for FABS/NBI calibration. The laser is directed to TCC from outside the target chamber. It then reflects from two mirrors (one of them is remotely pointed) into one of the FABS beams providing a complete *in-situ* calibration of the FABS. A quarter-wave plate is used to rotate the laser polarization in increments of 10° while measuring the energy on the calibration spectrometer. The final instrument sensitivity used for experimental analysis is the average of the extremes over the range of polarizations. The Surelite laser is used to calibrate NBI the same way as is described in [17].

IV (c). Backscatter power uncertainty

The FABS and NBI systems contribute differently to the error in the total power measurement. The largest

error in FABS comes from approximating the transmission through the final laser turning mirror (LM8). Near 351 nm the transmission through the mirror is decreasing rapidly with decreasing wavelength. In addition, the transmission is significantly different between S and P-polarized light. The calibration of UV transmission through this mirror is taken to be the average transmission from 350 nm to 353 nm and the average of the S and P-polarizations. This gives a single transmission value with an uncertainty of ±18%. A similar approach is taken for the SRS; however, the variation in transmission with polarization and wavelength is smaller than in the UV giving a resulting SRS uncertainty of ±14%. Added to these transmissions is 8% error in the calibration of the fast diode/flattening filter combination and 4% error in the ND filter calibration. These uncertainties are not correlated so they add in quadrature giving ±17% for SRS and ±20% for SBS.

The NBI system has uncertainties that arise from calibration, temporal evolution, and analysis that interpolates and extrapolates to regions with no plate material. The calibration uncertainties are estimated to be ±5% and the analysis uncertainties are approximately ±8% based on studies using different analysis techniques. The temporal evolution of the NBI is estimated to have an error of ±10%. Additional uncertainty from filters is estimated to be ±4%. Combining these as uncorrelated errors gives ±14%.

The NBI typically represents 2/3 of the backscatter signal and the FABS is 1/3. Estimating the total uncertainty as the sum of FABS and NBI to obtain a worst case gives 20%/3 + 2*14%/3 = ±16% which approximately meets the requirement. Different fractions of light into FABS and NBI as well as degradation in optics from debris or damage increases this error.

V. SUMMARY

Backscatter measurements on NIF utilize a FABS and an NBI instrument on two quads. A suite of detectors measures the energy, power and spectral content of the backscatter. Several methods are used to calibrate the power, energy, timing, sweep speed, and wavelength offset of the instruments. The power uncertainty is estimated to be ±16%. A new time-resolved NBI instrument shows that the overall time-history of the backscatter is very similar to the pulse shape obtained from the fast diode signals.

This work was performed under the auspices of the U. S. Department of Energy by the Lawrence Livermore National Laboratory under Contract No. DE-AC52-07NA27344.

* moody4@llnl.gov

[1] Glenzer, S. H. and MacGowan, B. J. and Michel, P. and Meezan, N. B. and Suter, L. J. and Dixit, S. N. and Kline, J. L. and Kyrala, G. A. and Bradley, D. K. and Callahan, D. A. and Dewald, E. L. and Divol, L. and Dzenitis, E. and Edwards, M. J. and Hamza, A. V. and Haynam, C. A. and Hinkel, D. E. and Kalantar, D. H. and Kilkenny, J. D. and Landen, O. L. and Lindl, J. D. and LePape, S. and Moody, J. D. and Nikroo, A. and Parham, T. and Schneider, M. B. and Town, R. P. J. and Wegner, P. and Widmann, K. and Whitman, P. and Young, B. K. F. and Van Wonterghem, B. and Atherton, L. J. and Moses, E. I., Science, **327**, 1228, 2010.

[2] E. I. Moses and C. I. Wuest, Fusion Science and Technology **47**, 314 (2005).

[3] J. D. Lindl, Phys. Plasmas **2**, 3933 (1995).

[4] Steven W. Haan, Stephen M. Pollaine, John D. Lindl, Laurance J. Suter, Richard L. Berger, Linda V. Powers, W. Edward Alley, Peter A. Amendt, John A. Futterman, W. Kirk Levedahl, Mordecai D. Rosen, Dana P. Rowley, Richard A. Sacks, Aleksei I. Shestakov, George L. Strobel, Max Tabak, Stephen V. Weber, and George B. Zimmerman, Phys. Plasmas **2**, 2480 (1995).

[5] R. K. Kirkwood, C. A. Back, M. A. Blain, D. E. Desenne, A. G. Dulieu, S. H. Glenzer, B. J. MacGowan, D. S. Montgomery, and J. D. Moody, Rev. Sci. Instrum., **68**, 636 (1997).

[6] J. M. Soures, R. L. McCrory, C. P. Verdon, A. Babushkin, R. E. Bahr, T. R. Boehly, R. Boni, D. K. Bradley, D. L. Brown, R. S. Craxton et al., Phys. Plasmas **3**, 2108 (1996).

[7] P. Neumayer, C. Sorce, D. H. Froula, L. Divol, V. Rekow, K. Loughman, R. Knight, S. H. Glenzer, R. Bahr, and W. Seka, Rev. Sci. Instrum., **79**, 10F548 (2008).

[8] D. H. Froula, D. Bower, M. Chrisp, S. Grace, J. H. Kamperschroer, T. M. Kelleher, R. K. Kirkwood, B. MacGowan, T. McCarville, N. Sewall, F. Y. Shimamoto, S. J. Shiromizu, B. Young, and S. H. Glenzer, Rev. Sci. Instrum., **75**, 4168 (2004).

[9] D. E. Bower, T. J. McCarville, S. S. Alvarez, L. E. Ault, M. D. Brown, M. P. Chrisp, C. M. Damian, W. J. DeHope, D. H. Froula, S. H. Glenzer, S. E. Grace, K. Gu, F. R. Holdener, C. K. Huffer, J. H. Kamperschroer, T. M. Kelleher, J. R. Kimbrough, R. Kirkwood, D. W. Kurita, A. P. Lee, F. D. Lee, I. T. Lewis, F. J. Lopez, B. J. MacGowan, M. W. Poole, M. A. Rhodes, M. B. Schneider, N. R. Sewall, F. Y. Shimamoto, S. J. Shiromizu, D. Voloshin, A. L. Warrick, C. R. Wendland, and B. K. Young, Rev. Sci. Instrum., **75**, 4177 (2004).

[10] R. K. Kirkwood, T. Mccarville, D. H. Froula, B. Young, D. Bower, N. Sewall, C. Niemann, M. Schneider, J. Moody, G. Gregori, F. Holdener, M. Chrisp, B. J. MacGowan, S. H. Glenzer, and D. S. Montgomery, Rev. Sci. Instrum., **75**, 4174 (2004).

[11] A. J. Mackinnon, T. McCarville, K. Piston, C. Niemann, G. Jones, I. Reinbachs, R. Costa, J. Celeste, G. Holtmeier, R. Griffith, R. Kirkwood, B. MacGowan, S. H. Glenzer, and M. R. Latta, Rev. Sci. Instrum., **75**, 4183 (2004).

[12] A. J. Mackinnon, C. Niemann, K. Piston, G. Holtmeier, T. McCarville, G. Jones, I. Reinbachs, R. Costa, J. Ce-

leste, R. Grifth, R. K. Kirkwood, B. J. MacGowan, and S. H. Glenzer, Rev. Sci. Instrum., **77**, 10E529 (2006).

[13] D. S. Montgomery and R. P. Johnson, Rev. Sci. Instrum., **72**, 979 (2001).

[14] Advanced Thin Films, 5733 Central Avenue, Boulder, CO 80301, Tel: 303-815-1545, FAX: 720-652-9948, web: http://www.atfilms.com.

[15] Electro-Optics Technology, Inc., 5835 Shugart Lane, Traverse City, MI. 49684 USA, Phone: +1 231 935 4044, Fax: +1 231 935 4046, US Free: 800-697-6782, E-mail: saleseotech.com, Web Address: www.eotech.com.

[16] R. A. London, D. H. Froula, C. M. Source, J. D. Moody, L. J. Suter, S. H. Glenzer, O. S. Jones, N. B. Meezan, and M. D. Rosen, Rev. Sci. Instrum., **79**, 10F549 (2008).

[17] P. Neumayer, C. Source, D. H. Froula, L. Divol, V. Rekow, K. Loughman, R. Knight, S. H. Glenzer, R. Bahr, and W. Seka, Rev. Sci. Instrum., **79**, 10F548 (2008).

[18] See for example: http://www.newport.com/Pencil-Style-Calibration-Lamps/377846/1033/catalog.aspx.